ACS OMEGA

Article

Cite This: ACS Omega 2019, 4, 12156−12166

http://pubs.acs.org/journal/acsodf

Amorphous TiO_2 Nanotubes as a Platform for Highly Selective Phosphopeptide Enrichment

Rudolf Kupcik,[†] Jan M. Macak,[‡,§] Helena Rehulkova,[∥] Hanna Sopha,[‡,§] Ivo Fabrik,[∥] V. C. Anitha,[‡] Jana Klimentova,[∥] Pavla Murasova,[†] Zuzana Bilkova,[†] and Pavel Rehulka*[,∥]

[†]Department of Biological and Biochemical Sciences, Faculty of Chemical Technology, University of Pardubice, Studentska 573, 532 10 Pardubice, Czech Republic

[‡]Center of Materials and Nanotechnologies, Faculty of Chemical Technology, University of Pardubice, Nam. Cs. Legii 565, 530 02 Pardubice, Czech Republic

[§]Central European Institute of Technology, Brno University of Technology, Purkynova 123, 612 00 Brno, Czech Republic

[∥]Department of Molecular Pathology and Biology, Faculty of Military Health Sciences, University of Defence, Trebesska 1575, 500 01 Hradec Kralove, Czech Republic

Supporting Information

ABSTRACT: This work reports highly selective phosphopeptide enrichment using amorphous TiO_2 nanotubes (TiO_2NTs) and the same material decorated with superparamagnetic Fe_3O_4 nanoparticles (TiO_2NTs@Fe_3O_4NPs). TiO_2NTs and TiO_2NTs@Fe_3O_4NPs materials were applied for phosphopeptide enrichment both from a simple peptide mixture (tryptic digest of bovine serum albumin and α-casein) and from a complex peptide mixture (tryptic digest of Jurkat T cell lysate). The obtained enrichment efficiency and selectivity for phosphopeptides of TiO_2NTs and TiO_2NTs@Fe_3O_4NPs were increased to 28.7 and 25.3%, respectively, as compared to those of the well-established TiO_2 microspheres. The enrichment protocol was extended for a second elution step facilitating the identification of additional phosphopeptides. It further turned out that both types of amorphous TiO_2 nanotubes provide qualitatively new physicochemical features that are clearly advantageous for highly selective phosphopeptide enrichment. This has been confirmed experimentally resulting in substantial reduction of non-phosphorylated peptides in the enriched samples. In addition, TiO_2NTs@Fe_3O_4NPs combine high selectivity and ease of handling due to the superparamagnetic character of the material. The presented materials and performances are further promising for applications toward a whole range of other types of biomolecules to be treated in a similar fashion.

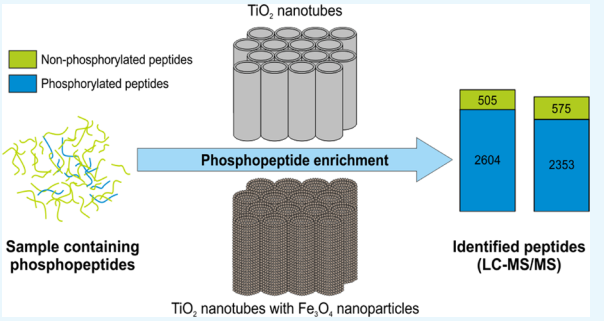

INTRODUCTION

Nanomaterials undoubtedly represent the most investigated group of materials. Many nanomaterials have already found major applications in life science and biomedical devices. In particular, functionalized nano/microstructures are not only widely used in biomedical and biochemical research but also gradually becoming an integral part of many diagnostic or therapeutic tools used in clinical practice.[1,2] Some of these materials have been fully exploited in the analysis of biological samples, especially for ultrahigh-throughput and parallel analysis at single-molecule levels. For example, in proteomics, nanomaterials are applied in the preanalytical enrichment phase combined with subsequent analysis of posttranslational modifications of proteins/peptides.[3]

Phosphorylation is a reversible covalent modification of proteins/peptides through which the protein/peptide function is regulated in response to extracellular stimuli.[4] Because phosphate groups carry highly negative charges, the phosphorylation of a protein can substantially change its conformation, which further affects the biological function, stability, and/or localization of the protein as well as its interaction with other proteins.[5] One of the major goals in phosphoproteomics, the field that studies the dynamic changes of phosphoproteins over time, is to identify and describe the relationship of the phosphorylation regulation with the mechanism and pathogenesis of many serious diseases.[6−8]

The analysis of phosphopeptides by mass spectrometry has many pitfalls that often distort the results and even lead to wrong conclusions. The low abundance of phosphopeptides, their low ionization efficiency, the labile phosphate moiety, and the interference of non-phosphorylated peptides strongly limit the comprehensive characterization of protein phosphorylation using mass spectrometry.[9−11] These problems are often addressed by a three-step approach: (i) enrichment of

Received: February 28, 2019
Accepted: June 21, 2019
Published: July 15, 2019

phosphopeptides and (ii) fractionation of phosphopeptides by liquid chromatography, which is then (iii) coupled with tandem mass spectrometry (LC−MS/MS).[12] Over the past years, many approaches, including the commonly used immobilized metal ion affinity chromatography (IMAC)[13,14] and metal oxide affinity chromatography (MOAC),[15−17] have been developed in order to specifically enrich phosphopeptides before their analysis by LC−MS/MS. The principle of the phosphopeptide enrichment by IMAC is based on the high affinity of the negatively charged and hydrophilic phosphate group to metal ions (e.g., Fe^{3+} and Ga^{3+}) immobilized on a chelating iminodiacetic or nitrilotriacetic acid. Although this method is selective and generally sensitive enough, it still suffers from a lower affinity for some phosphopeptides and is too susceptible to sample contaminants, for example, nucleic acids.[14] In addition, the non-specific adsorption of acidic peptides and peptides containing histidine may reduce the specificity of phosphopeptide enrichment.[18] While conventional immobilized metal ions in IMAC are mainly trivalent (Fe^{3+}/Al^{3+}/Ga^{3+}), tetravalent IMAC utilizes Zr^{4+}/Ti^{4+}/Ce^{4+} ions and commonly a phosphonate binding chemistry.[19−21] Like the TiO_2-based one, Ti^{4+}−phosphonate IMAC has a high tolerance toward acidic buffers to allow the enrichment of more basic phosphopeptides.[22] Nevertheless, IMAC utilizing Ti^{4+} has lower affinity toward the multiply phosphorylated peptides, as compared to conventional Fe^{3+}-IMAC enrichment.[23]

In the enrichment of phosphopeptides by metal oxides, the specificity has been substantially improved by introducing hydroxy acids such as 2,5-dihydroxybenzoic acid (DHB),[15] glutamic acid,[24] or lactic acid[25] in the loading and washing buffer. Since the introduction of effective phosphopeptide enrichment using DHB as the excluder for TiO_2 microspheres,[15] many metal oxides have been successfully applied in the enrichment of phosphopeptides, either as metal oxides (ZrO_2, Fe_3O_4, Al_2O_3, SnO_2, HfO_2, or CeO_2)[26−31] or composite materials (e.g., TiO_2−ZrO_2 and CeO_2−ZrO_2 composites).[32,33] The review of Wang et al.[3] provides a well-organized summary of materials developed and applied for phosphorylated protein/peptide enrichment. Despite this progress, however, the development of metal oxide-based affinity materials for the specific enrichment of phosphopeptides is still an ongoing process. Some of the reported studies only tested simple model mixtures of defined proteins rather than real complex samples like cell lysates.[3,32−34] Therefore, it is necessary to acquire suitable materials and to design a protocol that could effectively treat also the real complex peptide mixtures often analyzed in various biological studies.

A very promising example of material that could be very effective for the purification represents self-organized TiO_2 nanotubes prepared by anodization of titanium. These nanotubes possess many intriguing properties, such as their unique 1D structure, tunability of dimensions, stability, biocompatibility, and easy preparation.[35,36] Consequently, they have been applied in many different bioapplications for the photocatalytic killing of cancer cells,[37] drug delivery,[38] biosensing,[39] protein adsorption and separation,[40,41] and His-tagged protein purification.[42] Surprisingly, the potential of TiO_2 nanotubes for phosphopeptide enrichment was only noticed recently, starting with the introduction of tunable TiO_2 nanotube arrays either directly incorporated into the microchip for on-chip enrichment of serum phosphopeptides[43] or nanotubes grown on a titanium wire.[44] The materials can be further made magnetically active by utilizing the superparamagnetic properties of magnetic components (e.g., Fe_3O_4, γ-Fe_2O_3).[42,45] Consequently, these composite materials can be rapidly isolated with an external magnetic field and easily dispersed, greatly facilitating the separation procedure by reducing the loss of affinity materials and biological samples, factors that directly impact the enrichment efficiency.[3] Magnetic affinity composites are usually core−shell structures where the magnetic core does not interact with the surrounding environment. Anodic TiO_2 nanotubes decorated by Fe_3O_4 nanoparticles represent an interesting composite material that can be easily manipulated using an external magnetic field and possesses unique features usable for various bioapplications. We have recently shown that this material can be directly engaged in affinity interactions for the isolation of His-tagged recombinant proteins.[42] However, this material has great potential for the treatment of other biomolecules, which is demonstrated in the presented study in the case of phosphopeptides.

In this work, we introduce amorphous TiO_2 nanotubes (TiO_2NTs) and amorphous TiO_2 nanotubes decorated with superparamagnetic Fe_3O_4 nanoparticles (TiO_2NTs@Fe_3O_4NPs) as innovative materials for the enrichment of phosphopeptides. The tryptic digests of standard proteins as well as of highly complex cell lysates were utilized for the demonstration of phosphopeptide enrichment performance of the TiO_2NTs and TiO_2NTs@Fe_3O_4NPs materials. In addition, we developed a two-step sequential elution procedure resulting in an increased number of the detected phosphopeptides for all tested materials.

MATERIALS AND METHODS

Preparation of TiO_2NTs and TiO_2NTs@Fe_3O_4NPs. TiO_2NTs and TiO_2NTs@Fe_3O_4NPs materials were prepared as described in our previous work.[42] Commercially available TiO_2 microspheres with a nominal diameter of 10 μm (Titansphere, GL Sciences) were used as a reference. Morphological characterizations of materials were performed using a field emission scanning electron microscopy (SEM) system (JSM 7500F, JEOL Ltd.). The structure of the samples was analyzed by diffraction analyses using an X-ray diffractometer (Empyrean, Panalytical) with Cu Kα radiation. The specific surface area and the pore size distribution of TiO_2NTs, TiO_2NTs@Fe_3O_4NPs, and TiO_2 microspheres were determined according to the N_2 adsorption isotherms. Measurements of adsorption isotherms of nitrogen (purity, 99.999 vol %) were carried out using an ASAP 2020 and evaluated using the MicroActive software (Micromeritics, USA). Specific surface areas were calculated from nitrogen adsorption isotherms using the BET approach.[46] Pore size distributions were determined by means of the BJH method[47] using the Harkins−Jura equation to calculate the adsorbed layer thickness.[48]

Preparation of Model Phosphopeptide Mixtures. Tryptically digested phosphoprotein α-casein and bovine serum albumin were used as a simple model peptide mixture. Both proteins were resuspended in 50 mM NH_4HCO_3. A given amount of dithiothreitol (DTT) was added to reach the final concentration of 20 mM, and the solution was incubated for 30 min at 56 °C. Then, iodoacetamide (IAA) was added to the final concentration of 40 mM, and the solution was incubated for 30 min protected from light at RT. Alkylation was quenched by raising the DTT concentration to 40 mM.

DOI: 10.1021/acsomega.9b00571
ACS Omega 2019, 4, 12156−12166

The protein was digested with sequencing-grade modified trypsin (Promega, USA) at 37 °C overnight using an enzyme/substrate ratio of 1:50 (w/w).

For the preparation of the complex peptide mixture, Jurkat T cells were cultivated in RPMI-1640 medium with 10% (v/v) fetal bovine serum (FBS, Sigma-Aldrich, USA) at 37 °C/5% CO_2 and passaged every 2 or 3 days. The harvested cells were first treated with 1 mM pervanadate for 10 min at 37 °C (3.5×10^7 cells/mL),[49] then resuspended in an ice-cold hypotonic lysis buffer (10 mM Tris at pH 7.5 and 0.5 mM $MgCl_2$), and lysed using a glass Dounce homogenizer with a tight pestle (20 strokes). The protein concentration in the lysate was measured using a Micro BCA kit (Thermo Pierce, USA). The proteins were reduced by the addition of DTT (final concentration, 10 mM) and left for 1 h at 37 °C followed by alkylation with IAA (final concentration 20 mM) for 30 min at RT in the dark. An excess of IAA was quenched by the addition of DTT to the final concentration of 20 mM, and the reaction mixture was left for 15 min at RT. The proteins were digested by TCPK-treated trypsin from bovine pancreas (Sigma-Aldrich, USA) at an enzyme/substrate ratio of 1:50 (w/w) at 37 °C overnight. The peptides were desalted on Discovery DSC-18 SPE cartridges (500 mg/3 mL, Sigma-Aldrich, USA), eluted with 80% acetonitrile (ACN)/0.1% trifluoroacetic acid (TFA) and vacuum-dried.

Phosphopeptide Enrichment. Phosphopeptide enrichment was performed with either TiO_2NTs, TiO_2NTs@Fe_3O_4NPs, or commercial TiO_2 microspheres. Phosphopeptide enrichment was carried out for both simple and complex peptide mixtures following the previously reported protocols[25,50,51] and extended for the second elution step in order to obtain higher phosphoproteome coverage. To optimize the binding and elution conditions, tryptically digested α-casein (20 pmol) and bovine serum albumin (BSA, 200 pmol) were used as a simple model mixture, and the resulting protocol was performed also for the complex peptide mixture. The complex peptide mixture was enriched in duplicate, and each elution fraction was measured twice by nanoLC−MS/MS. Each material (3 mg of TiO_2NTs, TiO_2NTs@Fe_3O_4NPs, or TiO_2 microspheres) was dispersed separately in 80% ACN/0.1% TFA (v/v) in Eppendorf tubes and washed with 80% ACN/5% TFA (v/v) containing 1 M lactic acid. Dried tryptically digested whole cell lysates of Jurkat T cells (500 μg) were reconstituted in a loading buffer of 80% ACN/5% TFA (v/v) containing 1 M lactic acid, loaded onto the washed material for 30 min, and the supernatant was saved for a further re-enrichment step. Each material was then sequentially washed twice with 80% ACN/5% TFA (v/v) containing 1 M lactic acid, twice with 80% ACN/5% TFA (v/v), and once with 20% ACN/0.5% TFA (v/v). Phosphopeptides were eluted from the material using 1% NH_4OH (first elution step) followed by elution with 3% NH_4OH/45% ACN (v/v) containing 50 mM $(NH_4)_2HPO_4$ (second elution step). Supernatant fractions from TiO_2NTs and TiO_2NTs@Fe_3O_4NPs saved after the loading step were re-enriched using 3 mg of TiO_2 microspheres with the same protocol utilized for the raw lysate digest enrichment. The pH of all the elution fractions was reduced to 2−3 with 20% TFA. Prior to nanoLC−MS analysis, the elution fractions were desalted using custom-made reversed-phase microcolumns (length, 10 mm; ID, 250 μm) packed with 2.6 μm Kinetex EVO C18 resin (Phenomenex, USA) in FEP (fluorinated ethylene propylene) tubing (VICI AG, Switzerland) blocked with a small piece of Whatman glass microfiber filter (GE Healthcare, USA). Samples eluted with a non-linear gradient with gradually increasing ACN content (2−40% ACN/0.1% TFA) from the desalting microcolumns were dried using a vacuum concentrator (Eppendorf, Germany) and frozen.[52,53]

Mass Spectrometric Analysis. Mass spectrometric analysis of the simple mixture following enrichment was performed on the MALDI LTQ Orbitrap XL mass spectrometer (Thermo Fisher Scientific, USA) with DHB solution (10 g L^{-1} in 50% ACN/0.1% TFA) with 1% H_3PO_4 as a matrix.[15] Data were acquired in positive mode with full MS scan (800−4000 m/z) at 60,000 FWHM.

Peptides from the complex mixtures were first dissolved in 20 μL of 2% ACN/0.1% TFA, and 1 μL was analyzed using an UltiMate 3000 HPLC system (Dionex, USA) including a μ-Precolumn (300 μm × 5 mm, C_{18}PepMap 5 μm 100 Å particles; Dionex, USA) connected to an analytical NanoEase column (100 μm × 150 mm, Atlantis C_{18} 3 μm 100 Å particles; Waters, USA). The separation was performed with a bilinear gradient of 5−45% ACN/0.1% TFA over 81 min under a flow rate of 360 nL min^{-1} and UV detection set to 215 nm. The separation of peptides for nanoLC-MS/MS analysis was done using the UltiMate 3000 RSLC-nano HPLC system (Dionex, USA) with a trap column (75 μm × 20 mm) packed with 3 μm Acclaim PepMap100 C18 particles and a separation column (75 μm × 150 mm) packed with 2 μm Acclaim PepMap RSLC C18 particles. The separation was performed with a dual linear gradient using 3−44% ACN over 89 min under a flow rate of 300 nL min^{-1} and analyzed with a Q Exactive system (Thermo Fisher Scientific, USA) in positive mode with full MS scan (350−1650 m/z) at 70,000 FWHM and with the top 12 precursors in MS/MS at 17,500 FWHM. Proteome Discoverer software (Thermo Fisher Scientific, USA, version 2.2.0.388) connected to the Mascot searching engine (version 2.4.1) was used for identification of MS/MS spectra. The parameters for Mascot database searching were as follows: instrument, ESI-QUAD-TOF; protein database, UniProt human reference proteome UP000005640 (July 5, 2018); enzyme, trypsin; maximum missed cleavage sites, 2; taxonomy, all entries; precursor mass tolerance, 15 ppm; fragment mass tolerance, 20 mmu; static modification, carbamidomethyl (C); dynamic modifications − oxidation (M), acetyl (protein N-term), Gln- > pyro-Glu (N-term Q), Glu- > pyro-Glu (N-term E), pyro-carbamidomethyl (N-term C), phospho (ST), phospho (Y).

The statistical language R (version 3.5.0)[54] with RStudio interface (version 1.1.447) and pre-programmed Excel (Microsoft, USA) worksheets were used for processing the results exported from Proteome Discoverer software. The MS proteomics data were deposited to the ProteomeXchange Consortium via the PRIDE partner repository with the dataset identifier PXD012749 (DOI: 10.6019/PXD012749).

RESULTS AND DISCUSSION

TiO_2NTs, TiO_2NTs@Fe_3O_4NPs, and TiO_2 Microspheres for Phosphopeptide Enrichment. One of the developed materials, TiO_2NTs@Fe_3O_4NPs, was recently described and characterized by SEM, STEM, and magnetic measurements in our previous work.[42] In this work, TiO_2 nanotubes without Fe_3O_4 nanoparticle loading (noted as TiO_2NTs) were also employed for the evaluation of phosphopeptide enrichment capabilities. For the characterization of the materials, X-ray diffraction (XRD), specific surface area measurements, and

DOI: 10.1021/acsomega.9b00571
ACS Omega 2019, 4, 12156−12166

SEM analyses were performed. Figure 1a,b shows SEM images of TiO_2 microspheres as the reference material for phosphopeptide enrichment, and Figure 1c,d shows SEM images of the as-prepared amorphous TiO_2NTs with an internal diameter of ~230 nm at two different magnifications. In the next step, the TiO_2NTs were homogeneously decorated with magnetite nanoparticles to yield TiO_2NTs@Fe_3O_4NPs. Figure 1e,f confirms the presence of a homogeneous decoration of TiO_2NTs with magnetite nanoparticles, and this material was further used as a superparamagnetic material for phosphopeptide enrichment utilizing also the interactions of phosphopeptides with Fe_3O_4 nanoparticles on the surface of the composite TiO_2NTs@Fe_3O_4NP material.

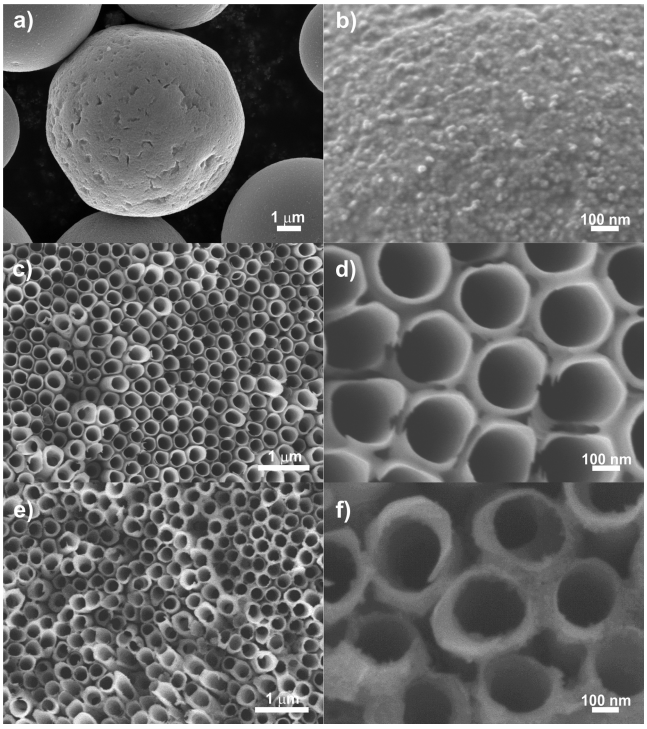

Figure 1. SEM images of (a, b) TiO_2 microspheres, (c, d) TiO_2NT layers, and (e, f) TiO_2NTs@Fe_3O_4NP layers at different magnifications.

To analyze the crystalline structure of tested materials, X-ray diffraction (XRD) analyses have been performed (Figure S-1). XRD patterns revealed that both types of TiO_2NTs remained amorphous after drying at 60 °C for 4 h and that commercial TiO_2 microspheres possess a tetragonal anatase crystalline structure.

The characterization of specific surface area (S_{BET}) using nitrogen adsorption/desorption isotherms of all three materials showed a substantial difference between both types of TiO_2NTs and the TiO_2 microspheres. The TiO_2 microspheres have a mesoporous structure, and S_{BET} was determined to be 127.5 ± 0.8 m^2 g^{-1}. This is a >5-fold higher value as compared to that of TiO_2NTs@Fe_3O_4NPs for which S_{BET} was determined to be 24.2 ± 0.3 m^2 g^{-1} and ~8.5 times higher than that for TiO_2NTs with 15.3 ± 0.2 m^2 g^{-1}. No porosity in the micro- and/or mesoporous range was observed for any TiO_2NT sample. According to the differences in the surface area of the materials, the maximum capacity for binding of phosphopeptides to TiO_2NTs and TiO_2NTs@Fe_3O_4NPs was assumed to be lower, and thus the enrichment efficiency was further compared for all three materials.

Workflow and Principles of Phosphopeptide Enrichment. According to the literature, TiO_2 and Fe_3O_4 are capable of selective interaction with phosphopeptides;[15,55] our TiO_2NTs consist of amorphous TiO_2, and they are strongly hydroxylated on the surface. Two additional interesting specific features are combined within TiO_2NTs@Fe_3O_4NPs: the unique morphology of strongly hydroxylated amorphous nanotubes along with the superparamagnetic property of the particles. Therefore, both materials should be capable of phosphopeptide adsorption and their enrichment from peptide mixtures. To verify that, two different samples were used to test the phosphopeptide enrichment by the TiO_2NTs and TiO_2NTs@Fe_3O_4NP materials: the simple peptide mixture containing digests of BSA and α-casein and the complex peptide mixture derived from whole cell lysates of Jurkat T cells. The overall enrichment performance of TiO_2NTs and TiO_2NTs@Fe_3O_4NP materials was also compared to the well-established phosphopeptide enrichment using TiO_2 microspheres.

Figure 2 schematically depicts the experimental workflow for the phosphopeptide enrichment using either TiO_2NTs or TiO_2NTs@Fe_3O_4NPs (Figure 2a) and TiO_2 microspheres as a reference (Figure 2b). The same separation conditions for the enrichment and effective isolation of singly and multiply phosphorylated peptides were essentially used for all three materials. To estimate the efficiency of phosphopeptide enrichment, the TiO_2 microspheres were also used for the re-enrichment of supernatant fractions resulting from enrichment of the complex peptide mixture with TiO_2NTs or TiO_2NTs@Fe_3O_4NPs. The second (additional) elution step was included in the protocol directly after the first elution step in order to obtain the phosphopeptides remaining on the material. The enrichment of the simple peptide mixture was assessed by MALDI-MS analysis, while for the complex peptide mixture, the nanoLC-MS/MS analysis was used. Separation of the TiO_2NTs and the TiO_2 microspheres from the liquid phase was done by centrifugation at 3000*g*, whereas TiO_2NTs@Fe_3O_4NPs were quickly and easily separated using a Nd magnet. The magnetic features of the TiO_2NTs@Fe_3O_4NPs allow faster and easier handling that is especially useful in parallel processing of several samples. Furthermore, the liquid–solid separation is more quantitative for the TiO_2NTs@Fe_3O_4NPs due to the low liquid retention in the test tube within replacement of individual solutions, which reduces the liquid carryover to the following steps.

Enrichment of Phosphopeptides from the Simple Peptide Mixture. To preliminarily evaluate the phosphopeptide enrichment ability of TiO_2NTs and TiO_2NTs@Fe_3O_4NPs, the standard simple peptide mixture containing tryptic digests of α-casein and BSA in a molar ratio of 1:10 was utilized. Phosphopeptides originating from α-casein were enriched using the protocol described schematically in Figure 2a. The obtained (phospho)peptide mixture was directly analyzed using a MALDI-Orbitrap MS. The MALDI spectrum of the original peptide mixture (Figure 3a) contains almost no apparent signal of phosphopeptides, while the first eluents from the sample enriched with either TiO_2NTs (Figure 3b), TiO_2NTs@Fe_3O_4NPs (Figure 3d), or TiO_2 microspheres (Figure 3f) contain intensive signals of phosphopeptides. This confirms the ability of TiO_2NTs and TiO_2NTs@Fe_3O_4NPs to enrich phosphopeptides from peptide mixtures in a similar way

DOI: 10.1021/acsomega.9b00571
ACS Omega 2019, 4, 12156−12166

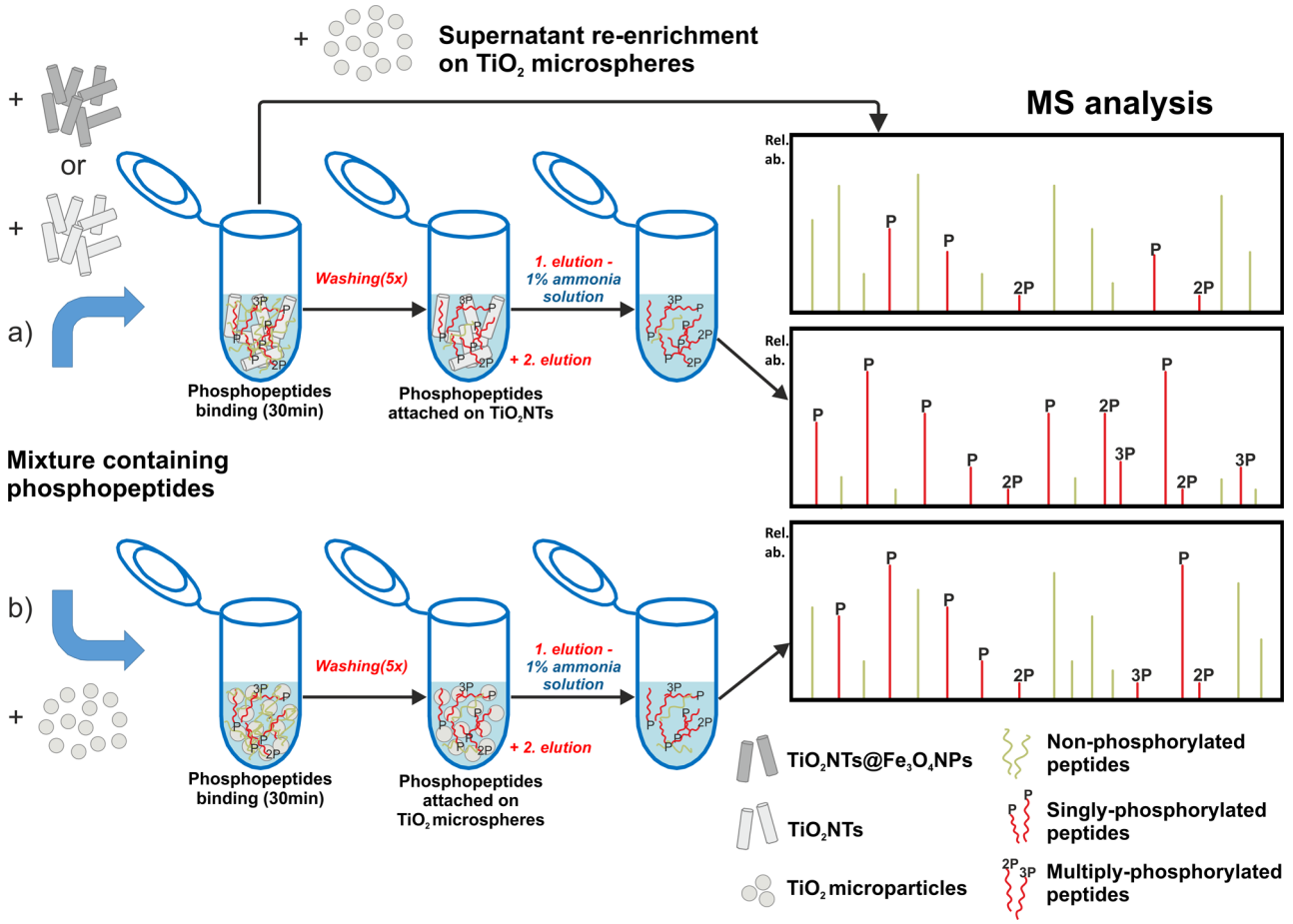

Figure 2. Schematic representation of the phosphopeptide enrichment workflow applied in this study using (a) TiO_2NTs or TiO_2NTs@Fe_3O_4NPs and (b) TiO_2 microspheres. Aliquots of tryptic digests of both standard proteins and complex cell lysates were used for the direct comparison of tested material.

as is usually done with TiO_2 microspheres. The amount of non-phosphorylated peptides observed in the first elution fraction is comparable for both TiO_2NTs or TiO_2NTs@Fe_3O_4NPs (Figure 3b,d) and TiO_2 microspheres (Figure 3f). The second elution fraction from TiO_2 microspheres (Figure 3g) contained a slightly higher abundance of non-specifically bound peptides (mainly in the range of m/z 700−1100) as compared to the second elution fraction from TiO_2NTs (Figure 3c) or TiO_2NTs@Fe_3O_4NPs (Figure 3e). Furthermore, the second elution fractions of all three materials (Figure 3c,e,g) showed a relative increase in signal abundance of multiply phosphorylated peptides. These differences between the first and the second elution fractions may be explained by the improved elution characteristics of the 3% NH_4OH/45% ACN (v/v) solution containing 50 mM $(NH_4)_2HPO_4$. This led us to further evaluate whether the second elution step could be possibly helpful in the analysis of multiply phosphorylated peptides. This might be important, for example, in studies focused on the analysis of hyperphosphorylated proteins related to certain pathology states.[7,8]

Enrichment of Phosphopeptides from the Complex Peptide Mixture. In common real samples used for phosphopeptide profiling (cell lysates, extracellular matrix, tissue extracts, etc.), the phosphorylation modification often appears with a very low stoichiometry, which makes the phosphorylation analysis very difficult. Therefore, these samples need highly selective and specific methods for phosphopeptide isolation in order to analyze the phosphopeptides successfully. Such methods should include both optimized sample processing conditions and suitable materials capable of handling the overwhelming sample complexity toward efficient phosphopeptide isolation. In this study, TiO_2NTs and TiO_2NTs@Fe_3O_4NPs were also tested for phosphopeptide isolation from the complex peptide mixture obtained as a tryptic digest of the whole cell lysate of Jurkat T cells treated with Na_3VO_4/H_2O_2.

For all materials, two enrichment replicates were analyzed, and nanoLC−MS/MS measurement of each replicate was performed in duplicate. Only peptides identified in both enrichment replicates and at least in one of two technical replicates with high confidence (1% FDR) were considered into the evaluation. Figure 4a shows a Venn diagram summarizing the number of phosphopeptides identified in the first elution fractions after phosphopeptide enrichment with TiO_2NTs, TiO_2NTs@Fe_3O_4NPs, or TiO_2 microspheres. As can be seen, the majority of the identified phosphopeptides are identical for all three materials. This shows a similar performance of all three tested materials. Nevertheless, from the number of uniquely identified phosphopeptides for particular materials, it is obvious that the materials are partially complementary in the phosphopeptide coverage and that the use of more different materials for phosphopeptide enrichment can be beneficial to a deeper phosphopeptide analysis of the sample. Although it is known that the number of identified

DOI: 10.1021/acsomega.9b00571
ACS Omega 2019, 4, 12156−12166

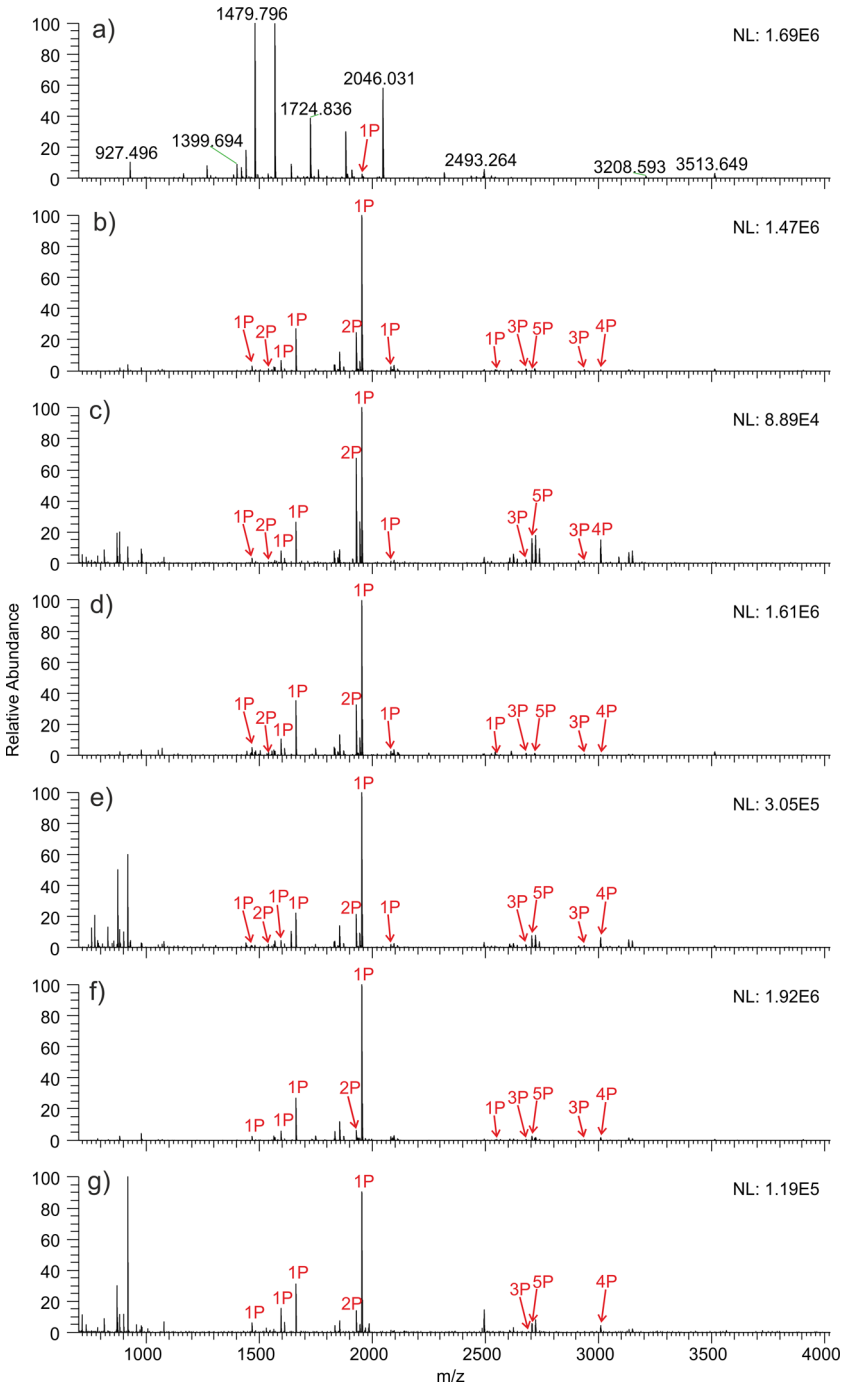

Figure 3. MALDI-Orbitrap mass spectra of tryptic peptides from α-casein and BSA. (a) Original peptide mixture, (b, c) first and second elution fraction after enrichment with TiO_2NTs, (d, e) first and second elution fraction after enrichment with TiO_2NTs@Fe_3O_4NPs, and (f, g) first and second elution fraction after enrichment with TiO_2 microspheres. Phosphopeptides are marked with the number of phosphates (P). Oxidized forms of marked phosphopeptides and in-source loss of phosphate groups from this phosphopeptides are not highlighted in the spectra to keep the figure simple.

phosphopeptides can be increased by multiple sample injections in LC−MS analysis (22.1 and 22.7% more phosphopeptides for two sample injections of TiO_2NTs and TiO_2NTs@Fe_3O_4NP phosphopeptide isolates, respectively), the substitution of a second sample injection in the case of both nanotube-based materials by injection of a phosphopeptide sample obtained with TiO_2 microspheres led to a slightly increased phosphopeptide identification rate (27.9 and 36.1% for TiO_2NTs and TiO_2NTs@Fe_3O_4NPs, respectively).

Figure 4b provides a summary overview of all identified phosphorylated and non-phosphorylated peptides in the first elution fraction for all materials. The total number of identified phosphopeptides was similar for both TiO_2NTs and TiO_2 microspheres (2604 and 2595, respectively), and it was slightly lower for TiO_2NTs@Fe_3O_4NPs (2353, i.e., ∼9.3% less phosphopeptides as compared to TiO_2 microspheres). However, a significant difference appeared between nanotube-based materials and TiO_2 microspheres in the number of

DOI: 10.1021/acsomega.9b00571
ACS Omega 2019, 4, 12156−12166

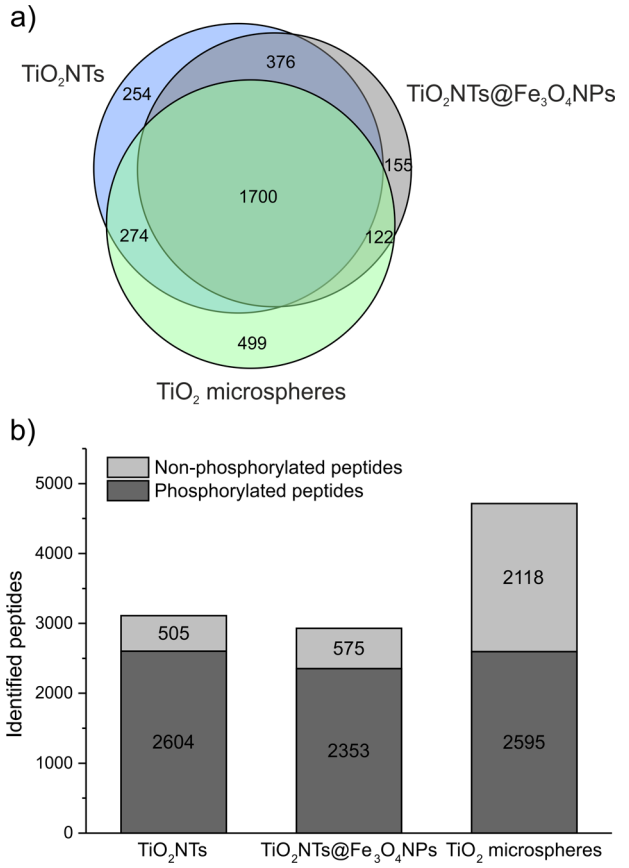

Figure 4. Comparison of the first elution fractions originating from the raw lysate digest enrichment using TiO_2NTs, TiO_2NTs@Fe_3O_4NPs, and TiO_2 microspheres. (a) Venn diagram of identified phosphopeptides for particular materials and (b) column diagram with total numbers of identified phosphorylated and non-phosphorylated peptides.

identified non-phosphorylated peptides in the first elution fractions. Here, TiO_2NTs and TiO_2NTs@Fe_3O_4NP materials showed a significantly lower proportion of non-phosphorylated peptides in all identified peptides (505 out of 3019, 16.2%, and 575 out of 2928, 19.6%, respectively), as compared to TiO_2 microspheres (2118 out of 4713, 44.9%). This clearly shows a significantly improved selectivity of TiO_2NTs and TiO_2NTs@Fe_3O_4NP materials compared to the TiO_2 microspheres for the phosphopeptide enrichment. The decrease of non-phosphorylated peptides in elution fractions has a positive impact on the enriched sample purity obtained mainly from highly complex samples containing phosphopeptides in low abundance. Increased non-specific sorption of non-phosphorylated peptides on TiO_2 microspheres was also obvious from nanoLC analysis with UV detection where a significantly higher UV response for the first elution fractions from TiO_2 microspheres was observed (Figure S-2). The improved selectivity of TiO_2NTs and TiO_2NTs@Fe_3O_4NPs is presumably caused by the corresponding material's composition, its structure, or non-crystallinity affecting its interaction with the peptides. Although the capacity of the nanotube-based materials for phosphopeptide enrichment proves to be comparable with TiO_2 microspheres under the used experimental conditions, further optimization of TiO_2NTs or TiO_2NTs@Fe_3O_4NPs is possible for an increased number of identified peptides while maintaining the superior material selectivity. This optimization includes in particular tailoring the aspect ratio of the nanotubes (i.e., the ratio between the tube length and inner diameter) and the surface hydroxylation.

Two-Step Phosphopeptide Elution and Analysis of Multiply Phosphorylated Peptides. MOAC phosphopeptide enrichment based on the use of TiO_2 is popular for its simplicity and relatively high specificity. However, multiply phosphorylated peptides are usually observed to a lower extent in the TiO_2-enriched peptide mixtures as compared to, for example, IMAC phosphopeptide enrichment. One assumption is that certain (especially multiply) phosphorylated peptides may not be eluted under standard elution conditions from TiO_2-based materials.[50] To address this point, an easy second elution step in addition to the standard phosphopeptide elution with ammonia solution was introduced to the enrichment protocol in this work. The composition of the second elution solution was given by an increased concentration of ammonia (3 vs 1% NH_4OH), the introduction of ACN (45%, v/v) to diminish the non-specific sorption of peptides on the material, and the addition of phosphate salt (50 mM $(NH_4)_2HPO_4$) for an increased competitive elution of phosphopeptides. This simple additional step follows the first elution step, and thus it does not have any effect on the results obtained with the standard elution procedure. The processing of the second eluent is almost the same as for the first with the exception of the vacuum drying step, included prior to the reversed-phase-based sample clean-up for the following nanoLC−MS/MS analysis.

The first test with the simple mixture of two standard proteins suggested that the relative abundance of multiply phosphorylated peptides may increase in the second elution fraction (Figure 3c,e,g). To verify these observations, the second elution step was also included in the analysis of complex peptide mixtures derived from Jurkat T cells for the compared materials. The UV records from nanoLC analysis for TiO_2NTs, TiO_2NTs@Fe_3O_4NPs, and TiO_2 microspheres (Figure S-3−S-5, respectively) confirm that the total peptide amount is significantly lower than that obtained in the first elution step. However, the following nanoLC-MS/MS analysis still identified a significant amount of phosphopeptides also in the second elution fractions (1785, 1188, and 1633 for TiO_2NTs, TiO_2NTs@Fe_3O_4NPs, and TiO_2 microspheres, respectively; Figure 5a). The vast majority of these identified phosphopeptides were also found in the nanoLC-MS/MS analysis of the first elution fraction as shown in the Venn diagrams in Figure 5b. Nevertheless, when compared to the number of phosphopeptides identified in the first elution fraction, 216, 204, and 265 phosphopeptides were newly identified for TiO_2NTs, TiO_2NTs@Fe_3O_4NPs, and TiO_2 microspheres comprising an increase of 8.3, 8.7, and 10.2% in the overall phosphopeptide coverage, respectively.

The obtained data for all materials and both elution fractions were also evaluated according to the number of phosphate groups on the peptide backbone present in identified phosphopeptides, and the summary is presented in the Table 1. From this point, all three materials are comparable with a slightly lower performance of TiO_2NTs, whereas TiO_2NTs@Fe_3O_4NPs show the highest ratio of multiply phosphorylated peptides toward singly phosphorylated ones. The hypothesis about the increased presence of multiply phosphorylated peptides in the second elution fraction was partially confirmed for TiO_2NTs@Fe_3O_4NPs where the relative ratio of multiply

DOI: 10.1021/acsomega.9b00571
ACS Omega 2019, 4, 12156−12166

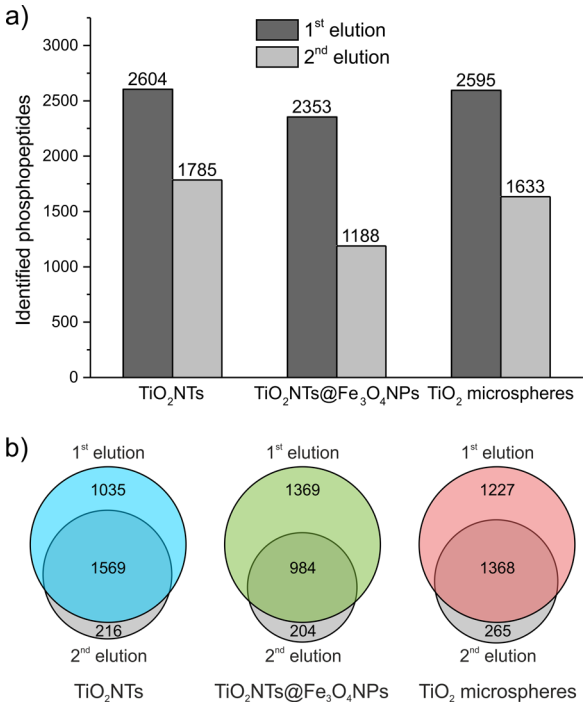

Figure 5. Comparison of the first and second elution fractions originating from the raw lysate digest enrichment using TiO_2NTs, TiO_2NTs@Fe_3O_4NPs, and TiO_2 microspheres. (a) Column diagram with total numbers of identified phosphopeptides and (b) Venn diagrams with intersections of both elution steps.

phosphorylated peptides was the highest among the materials and even increased in the second elution fraction.

Re-enrichment of Supernatant Fractions with TiO_2 Microspheres. To further characterize the phosphopeptide enrichment capabilities of TiO_2NTs and TiO_2NTs@Fe_3O_4NPs, the supernatant fraction from the complex peptide mixture enrichment with nanotube-based materials was re-enriched using TiO_2 microspheres. The aim was to determine the level of effectiveness of phosphopeptide capture of TiO_2NTs and TiO_2NTs@Fe_3O_4NPs and to test whether these materials are applicable to the enrichment of typical complex peptide mixtures originating from biological experiments. The results of these experiments are summarized in Figure S-6, which compares identified phosphopeptides and non-phosphorylated peptides both in the first elution fraction of raw lysate enrichment and in the first elution from the supernatant re-enrichment.

NanoLC reversed-phase analysis with UV detection showed a higher amount of peptides present in the elution fraction from the supernatant re-enrichment as compared to the first and second elution fractions from the raw lysate enrichment (Figures S-3 and S-4). The following nanoLC-MS/MS analysis revealed that the supernatant fractions contained a lower number of identified phosphopeptides (905 and 1188 for TiO_2NTs and TiO_2NTs@Fe_3O_4NPs, respectively), whereas many of them (85.0 and 73.6%, respectively) have already been identified in the first elution fraction from the raw lysate enrichment. On the other hand, the re-enrichment of supernatant fractions originating from TiO_2NTs and TiO_2NTs@Fe_3O_4NPs using commercial TiO_2 microspheres led to the identification of other 136 and 194 phosphopeptides not identified previously in the first elution fraction from the raw lysate enrichment. These results show that the phosphopeptide enrichment using nanotube-based materials is very effective even though the results confirmed partial orthogonality between the TiO_2 microspheres, nanotube-based materials TiO_2NTs, and TiO_2NTs@Fe_3O_4NPs. This phenomenon has already been observed in the comparison with the identified phosphopeptides in the first elution fractions after raw lysate enrichment for all materials (Figure 4a). Then, this partial alternative selectivity can be also used in the re-enrichment of supernatant fractions in order to obtain higher phosphoproteome coverage of the analyzed sample although it is more laborious than the approach with the second elution step described in the previous section.

The results of the supernatant fraction re-enrichment show that the presumption of significantly lower capacity of TiO_2NTs and TiO_2NTs@Fe_3O_4NPs was not true for these materials, sample amount, and conditions used in the enrichment protocol. The lower capacity was presumed based on specific surface area analysis showing the 8.5-fold and 5.3-fold lower surface area by material weight for TiO_2NTs and TiO_2NTs@Fe_3O_4NPs as compared to TiO_2 microspheres, respectively. Furthermore, in the re-enriched supernatant fractions obtained using TiO_2 microspheres, an ~8-fold higher amount of non-phosphorylated peptides was observed as compared with raw lysate enrichment (Figure S-6c). This is in line with the results presented in Figure 4 that show a lower selectivity of TiO_2 microspheres as related to nanotube-based materials, and it confirms the importance of selectivity in phosphopeptide enrichment for this type of sample. Obviously, the samples enriched with materials with a higher level of non-specific sorption (e.g., TiO_2 microspheres in this case) will result in an increased content of non-phosphorylated peptides in the elution fractions, further leading to the signal suppression of phosphopeptides in the MS analysis.

TiO_2NTs and TiO_2NTs@Fe_3O_4NPs differ from the commonly used crystalline TiO_2 microspheres in several aspects, which may be responsible for their different selectivities. In other studies with similar protocols for enrichment of phosphopeptides from complex mixtures, the overall selectivity of commercial crystalline TiO_2 microspheres

Table 1. Total Numbers of Identified Phosphopeptides in the Elution Fractions (EFs) Isolated from the Complex Peptide Mixture According to the Number of Phosphorylations per Peptide

sample	1 × phospho	2 × phospho	3 × phospho
TiO_2NTs – 1st EF	2464	140	0
TiO_2NTs – 2nd EF	1687	98	0
TiO_2NTs@Fe_3O_4NPs – 1st EF	2176	175	2
TiO_2NTs@Fe_3O_4NPs – 2nd EF	1087	101	0
TiO_2 microspheres – 1st EF	2417	177	1
TiO_2 microspheres – 2nd EF	1521	112	0

DOI: 10.1021/acsomega.9b00571
ACS Omega 2019, 4, 12156−12166

was found to be ~70.1% when DHB was used as an excluder[56] and 72.2% in the case of lactic acid, which served also for exclusion of non-phosphorylated peptides.[57] These numbers are higher than those observed for TiO_2 microspheres in this work (55.1%); however, both studies used diverse initial samples, a different sample-to-microsphere ratio, and a two-dimensional LC MS setup. Apart from crystalline microspheres, phosphopeptides can directly interact with the presented nanotubular materials not only via the available amorphous TiO_2 surface of nanotubes but also in the case of TiO_2NTs@Fe_3O_4NPs through the Fe_3O_4 nanoparticles attached on the nanotube TiO_2 walls. The binding characteristic of TiO_2 is described mainly as bidentate coordination of hydroxyl groups to positively polarized Ti(IV), which is responsible for the preferential capture and enrichment of phosphopeptides.[58,59] In the IMAC technology, Ti^{4+} ions are utilized for phosphopeptide enrichment as well as Fe^{3+} ions.[19] As part of the SIMAC protocol, the Fe^{3+} IMAC technology is also responsible for the improved enriching of the multiply phosphorylated peptides.[50] Moreover, bare Fe_3O_4 nanoparticles[55] and Fe_3O_4 nanoparticles incorporated in a polymer-based monolithic column[60] were previously utilized for the phosphopeptide enrichment. Compared to polymer compounds, inorganic supports, such as TiO_2, may be beneficial due to their stability in organic solvents (e.g., acetonitrile).[42] TiO_2 as a support is even more useful since it can also enrich the phosphopeptides. Compared to other primarily crystalline materials available today, TiO_2NTs and TiO_2NTs@Fe_3O_4NPs possess an amorphous structure with a high number of hydroxyl groups on the surface responsible for very good hydrophilicity of the material and easy wetting of nanotube interiors.[61]

TiO_2-based nanotubes have already been described for phosphopeptide enrichment previously.[43,44] However, the nanotubes presented by Wijeratne et al. differ in their crystalline structure because they were annealed and produced in the form of anatase, and therefore the efficacy of phosphopeptide enrichment was similar to commercial TiO_2 microspheres.[44] The inner nanotube diameter was also narrower, ~110 and ~45 nm.[43,44] The inner diameter is important for accessibility of nanotube interiors to phosphopeptides; thus, the wider inner diameter (~230 nm) of TiO_2NTs and TiO_2NTs@Fe_3O_4NPs and their amorphous character may be crucial for the phosphopeptide enrichment efficiency. On the other hand, the increased tube diameter means a lower surface/volume ratio and surface/weight ratio.

CONCLUSIONS

This paper reports the successful application of TiO_2NTs and TiO_2NTs@Fe_3O_4NP materials for phosphopeptide enrichment preferably suitable for complex biological samples. In addition, the improved enrichment protocol including a second elution step for more extensive identification of phosphopeptides is presented. By comparison of TiO_2NTs and TiO_2NTs@Fe_3O_4NPs along with a reference material based on TiO_2 microspheres, it can be concluded that the amorphous TiO_2 nanotubular surface and the superparamagnetic version decorated with the Fe_3O_4 nanoparticles specifically interact with phosphopeptides. The performance of presented materials was comparable with well-established commercial TiO_2 microspheres although these possess a several times higher surface area by material weight. Our results unambiguously confirmed that the main difference between nanotube-based materials and TiO_2 microspheres lies in a different proportion of the non-specific sorption. The amorphous character of TiO_2 nanotubes results in a significantly improved selectivity for phosphopeptide isolation and to an increased ratio of phosphopeptides to peptides in the enriched sample. Substantially improved selectivity of TiO_2NTs and TiO_2NTs@Fe_3O_4NPs for phosphopeptides is observed in the reduction of non-specific sorption of non-phosphorylated biomolecules, and the suppression of phosphopeptide signal within nanoLC-MS analysis is thus diminished. Furthermore, in the analysis of complex cell lysate digests, the introduction of the second elution step enhanced the overall phosphoproteome coverage in the sample. Finally, the added superparamagnetic properties of the TiO_2NTs@Fe_3O_4NPs are also important for the simplified sample handling during phosphopeptide enrichment.

ASSOCIATED CONTENT

Supporting Information

The Supporting Information is available free of charge on the ACS Publications website at DOI: 10.1021/acsomega.9b00571.

Additional information about the materials' characteristics, nanoLC-UV analysis, and results of nano-LC-MS (PDF)

AUTHOR INFORMATION

Corresponding Author

*E-mail: pavel.rehulka@unob.cz.

ORCID

Jan M. Macak: 0000-0001-7091-3022
Helena Rehulkova: 0000-0003-1220-6631
Pavel Rehulka: 0000-0003-3263-4107

Author Contributions

The manuscript was written through contributions of all authors. All authors have given approval to the final version of the manuscript.

Notes

The authors declare no competing financial interest.

ACKNOWLEDGMENTS

J.M.M., H.S., and V.C.A. gratefully acknowledge the support of the European Research Council (project no. 638857) and the Ministry of Education, Youth and Sports of the Czech Republic (project nos. LM2015082, LQ1601, and CZ.02.1.01/0.0/0.0/16_013/0001829). J.M.M., H.S., R.K., P.M., and Z.B. thank OP RDE project "Strengthening interdisciplinary cooperation in research of nanomaterials and their effects on living organisms" (reg. n. CZ.02.1.01/0.0/0.0/17_048/0007421). P.R., I.F., J.K., and H.R. thank the financial support from a long-term organization development plan from the Faculty of Military Health Sciences, University of Defence (Czech Republic). The authors also thank Mrs. Eliška Kročová and Mrs. Denisa Janebová for technical help with experiments. The authors also thank Mr. Luděk Hromádko for XRD measurements and Prof. Roman Bulánek for BET surface area analysis.

REFERENCES

(1) Wan, A. C. A.; Ying, J. Y. Nanomaterials for in situ cell delivery and tissue regeneration. *Adv. Drug Delivery Rev.* **2010**, *62*, 731−740.

DOI: 10.1021/acsomega.9b00571
ACS Omega 2019, 4, 12156−12166

(2) Holzapfel, B. M.; Wagner, F.; Martine, L. C.; Reppenhagen, S.; Rudert, M.; Schuetz, M.; Denham, J.; Schantz, J.-T.; Hutmacher, D. W. Tissue engineering and regenerative medicine in musculoskeletal oncology. *Cancer Metastasis Rev.* **2016**, *35*, 475−487.
(3) Wang, Z.-G.; Lv, N.; Bi, W.-Z.; Zhang, J.-L.; Ni, J.-Z. Development of the affinity materials for phosphorylated proteins/peptides enrichment in phosphoproteomics analysis. *ACS Appl. Mater. Interfaces* **2015**, *7*, 8377−8392.
(4) Knorre, D. G.; Kudryashova, N. V.; Godovikova, T. S. Chemical and functional aspects of posttranslational modification of proteins. *Acta Nat.* **2009**, 29−51.
(5) Johnson, L. N.; Barford, D. The effects of phosphorylation on the structure and function of proteins. *Annu. Rev. Biophys. Biomol. Struct.* **1993**, *22*, 199−232.
(6) Fabrik, I.; Link, M.; Putzova, D.; Plzakova, L.; Lubovska, Z.; Philimonenko, V.; Pavkova, I.; Rehulka, P.; Krocova, Z.; Hozak, P.; Santic, M.; Stulik, J. The early dendritic cell signaling induced by virulent *Francisella tularensis* strain occurs in phases and involves the activation of Extracellular Signal-Regulated Kinases (ERKs) and p38 in the later stage. *Mol. Cell. Proteomics* **2018**, *17*, 81−94.
(7) Perluigi, M.; Barone, E.; Di Domenico, F.; Butterfield, D. A. Aberrant protein phosphorylation in Alzheimer disease brain disturbs pro-survival and cell death pathways. *Biochim. Biophys. Acta* **2016**, *1862*, 1871−1882.
(8) Hromadkova, L.; Kupcik, R.; Vajrychova, M.; Prikryl, P.; Charvatova, A.; Jankovicova, B.; Ripova, D.; Bilkova, Z.; Slovakova, M. Kinase-loaded magnetic beads for sequential *in vitro* phosphorylation of peptides and proteins. *Analyst* **2018**, *143*, 466−474.
(9) Beltran, L.; Cutillas, P. R. Advances in phosphopeptide enrichment techniques for phosphoproteomics. *Amino Acids* **2012**, *43*, 1009−1024.
(10) Nühse, T. S.; Stensballe, A.; Jensen, O. N.; Peck, S. C. Large-scale analysis of *in vivo* phosphorylated membrane proteins by immobilized metal ion affinity chromatography and mass spectrometry. *Mol. Cell. Proteomics* **2003**, *2*, 1234−1243.
(11) Dephoure, N.; Gould, K. L.; Gygi, S. P.; Kellogg, D. R. Mapping and analysis of phosphorylation sites: A quick guide for cell biologists. *Mol. Biol. Cell* **2013**, *24*, 535−542.
(12) Tichy, A.; Salovska, B.; Rehulka, P.; Klimentova, J.; Vavrova, J.; Stulik, J.; Hernychova, L. Phosphoproteomics: Searching for a needle in a haystack. *J. Proteomics* **2011**, *74*, 2786−2797.
(13) Shen, F.; Hu, Y.; Guan, P.; Ren, X. Ti^{4+}-phosphate functionalized cellulose for phosphopeptides enrichment and its application in rice phosphoproteome analysis. *J. Chromatogr. B* **2012**, *902*, 108−115.
(14) Fíla, J.; Honys, D. Enrichment Techniques Employed in Phosphoproteomics. *Amino Acids* **2012**, *43*, 1025−1047.
(15) Larsen, M. R.; Thingholm, T. E.; Jensen, O. N.; Roepstorff, P.; Jørgensen, T. J. D. Highly selective enrichment of phosphorylated peptides from peptide mixtures using titanium dioxide microcolumns. *Mol. Cell. Proteomics* **2005**, *4*, 873−886.
(16) Cheng, G.; Wang, Z.-G.; Liu, Y.-L.; Zhang, J.-L.; Sun, D.-H.; Ni, J.-Z. Magnetic affinity microspheres with meso−/macroporous shells for selective enrichment and fast separation of phosphorylated biomolecules. *ACS Appl. Mater. Interfaces* **2013**, *5*, 3182−3190.
(17) Salovska, B.; Tichy, A.; Fabrik, I.; Rezacova, M.; Vavrova, J. Comparison of resins for metal oxide affinity chromatography with mass spectrometry detection for the determination of phosphopeptides. *Anal. Lett.* **2013**, *46*, 1505−1524.
(18) Neville, D. C. A.; Townsend, R. R.; Rozanas, C. R.; Verkman, A. S.; Price, E. M.; Gruis, D. B. Evidence for phosphorylation of serine 753 in CFTR using a novel metal-ion affinity resin and matrix-assisted laser desorption mass spectrometry. *Protein Sci.* **1997**, *6*, 2436−2445.
(19) Zhou, H.; Xu, S.; Ye, M.; Feng, S.; Pan, C.; Jiang, X.; Li, X.; Han, G.; Fu, Y.; Zou, H. Zirconium phosphonate-modified porous silicon for highly specific capture of phosphopeptides and MALDI-TOF MS analysis. *J. Proteome Res.* **2006**, *5*, 2431−2437.
(20) Zhou, H.; Ye, M.; Dong, J.; Han, G.; Jiang, X.; Wu, R.; Zou, H. Specific phosphopeptide enrichment with immobilized titanium ion affinity chromatography adsorbent for phosphoproteome analysis. *J. Proteome Res.* **2008**, *7*, 3957−3967.
(21) Li, Y.; Qi, D.; Deng, C.; Yang, P.; Zhang, X. Cerium ion-chelated magnetic silica microspheres for enrichment and direct determination of phosphopeptides by matrix-assisted laser desorption ionization mass spectrometry. *J. Proteome Res.* **2008**, *7*, 1767−1777.
(22) Zhou, H.; Low, T. Y.; Hennrich, M. L.; van der Toorn, H.; Schwend, T.; Zou, H.; Mohammed, S.; Heck, A. J. R. Enhancing the identification of phosphopeptides from putative basophilic kinase substrates using Ti (IV) based IMAC enrichment. *Mol. Cell. Proteomics* **2011**, *10*, M110.006452.
(23) Lai, A. C.-Y.; Tsai, C.-F.; Hsu, C.-C.; Sun, Y.-N.; Chen, Y.-J. Complementary Fe^{3+}- and Ti^{4+}-immobilized metal ion affinity chromatography for purification of acidic and basic phosphopeptides. *Rapid Commun. Mass Spectrom.* **2012**, *26*, 2186−2194.
(24) Wu, J.; Shakey, Q.; Liu, W.; Schuller, A.; Follettie, M. T. Global profiling of phosphopeptides by titania affinity enrichment. *J. Proteome Res.* **2007**, *6*, 4684−4689.
(25) Sugiyama, N.; Masuda, T.; Shinoda, K.; Nakamura, A.; Tomita, M.; Ishihama, Y. Phosphopeptide enrichment by aliphatic hydroxy acid-modified metal oxide chromatography for nano-LC-MS/MS in proteomics applications. *Mol. Cell. Proteomics* **2007**, *6*, 1103−1109.
(26) Wang, H.; Duan, Y.; Zhong, W. ZrO_2 Nanofiber as a Versatile Tool for Protein Analysis. *ACS Appl. Mater. Interfaces* **2015**, *7*, 26414−26420.
(27) Wei, J.; Ren, Y.; Luo, W.; Sun, Z.; Cheng, X.; Li, Y.; Deng, Y.; Elzatahry, A. A.; Al-Dahyan, D.; Zhao, D. Ordered mesoporous alumina with ultra-large pores as an efficient absorbent for selective bioenrichment. *Chem. Mater.* **2017**, *29*, 2211−2217.
(28) Choi, S.; Kim, J.; Cho, K.; Park, G.; Yoon, J. H.; Park, S.; Yoo, J. S.; Ryu, S. H.; Kim, Y. H.; Kim, J. Sequential Fe_3O_4/TiO_2 enrichment for phosphopeptide analysis by liquid chromatography/tandem mass spectrometry. *Rapid Commun. Mass Spectrom.* **2010**, *24*, 1467−1474.
(29) Sturm, M.; Leitner, A.; Smått, J.-H.; Lindén, M.; Lindner, W. Tin dioxide microspheres as a promising material for phosphopeptide enrichment prior to liquid chromatography-(tandem) mass spectrometry analysis. *Adv. Funct. Mater.* **2008**, *18*, 2381−2389.
(30) Nelson, C. A.; Szczech, J. R.; Dooley, C. J.; Xu, Q.; Lawrence, M. J.; Zhu, H.; Jin, S.; Ge, Y. Effective enrichment and mass spectrometry analysis of phosphopeptides using mesoporous metal oxide nanomaterials. *Anal. Chem.* **2010**, *82*, 7193−7201.
(31) Sun, S.; Ma, H.; Han, G.; Wu, R.; Zou, H.; Liu, Y. Efficient enrichment and identification of phosphopeptides by cerium oxide using on-plate matrix-assisted laser desorption/ionization time-of-flight mass spectrometric analysis. *Rapid Commun. Mass Spectrom.* **2011**, *25*, 1862−1868.
(32) Yan, J.; Li, X.; Cheng, S.; Ke, Y.; Liang, X. Facile synthesis of titania-zirconia monodisperse microspheres and application for phosphopeptides enrichment. *Chem. Commun.* **2009**, 2929−2931.
(33) Wu, J.-H.; Xiao, K.; Zhao, Y.; Zhang, W.-P.; Guo, L.; Feng, Y.-Q. Preparation and characterization of ceria-zirconia composite for enrichment and identification of phosphopeptides. *J. Sep. Sci.* **2010**, *33*, 2361−2368.
(34) Li, X.-S.; Yuan, B.-F.; Feng, Y.-Q. Recent advances in phosphopeptide enrichment: Strategies and techniques. *TrAC, Trends Anal. Chem.* **2016**, *78*, 70−83.
(35) Sopha, H.; Jäger, A.; Knotek, P.; Tesař, K.; Jarosova, M.; Macak, J. M. Self-organized anodic TiO_2 nanotube layers: Influence of the Ti substrate on nanotube growth and dimensions. *Electrochim. Acta* **2016**, *190*, 744−752.
(36) Oliveira, W. F.; Arruda, I. R. S.; Silva, G. M. M.; Machado, G.; Coelho, L. C. B. B.; Correia, M. T. S. Functionalization of titanium dioxide nanotubes with biomolecules for biomedical applications. *Mater. Sci. Eng., C* **2017**, *81*, 597−606.
(37) Kalbacova, M.; Macak, J. M.; Schmidt-Stein, F.; Mierke, C. T.; Schmuki, P. TiO_2 nanotubes: photocatalyst for cancer cell killing. *Phys. Status Solidi RRL* **2008**, *2*, 194−196.
(38) Wang, Q.; Huang, J.-Y.; Li, H.-Q.; Chen, Z.; Zhao, A. Z.-J.; Wang, Y.; Zhang, K.-Q.; Sun, H.-T.; Al-Deyab, S. S.; Lai, Y.-K. TiO_2

DOI: 10.1021/acsomega.9b00571
ACS Omega 2019, 4, 12156−12166

nanotube platforms for smart drug delivery: A review. *Int. J. Nanomed.* **2016**, *11*, 4819−4834.
(39) Terracciano, M.; Galstyan, V.; Rea, I.; Casalino, M.; De Stefano, L.; Sbervegleri, G. Chemical modification of TiO_2 nanotube arrays for label-free optical biosensing applications. *Appl. Surf. Sci.* **2017**, *419*, 235−240.
(40) Kulkarni, M.; Mazare, A.; Park, J.; Gongadze, E.; Killian, M. S.; Kralj, S.; von der Mark, K.; Iglič, A.; Schmuki, P. Protein interactions with layers of TiO_2 nanotube and nanopore arrays: Morphology and surface charge influence. *Acta Biomater.* **2016**, *45*, 357−366.
(41) Xu, J.; Yang, L.; Han, Y.; Wang, Y.; Zhou, X.; Gao, Z.; Song, Y.-Y.; Schmuki, P. Carbon-decorated TiO_2 nanotube membranes: A renewable nanofilter for charge-selective enrichment of proteins. *ACS Appl. Mater. Interfaces* **2016**, *8*, 21997−22004.
(42) Kupcik, R.; Rehulka, P.; Bilkova, Z.; Sopha, H.; Macak, J. M. New interface for purification of proteins: One-dimensional TiO_2 nanotubes decorated by Fe_3O_4 nanoparticles. *ACS Appl. Mater. Interfaces* **2017**, *9*, 28233−28242.
(43) Min, Q.; Chen, X.; Zhang, X.; Zhu, J.-J. Tailoring of a TiO_2 nanotube array-integrated portable microdevice for efficient on-chip enrichment and isotope labeling of serum phosphopeptides. *Lab Chip* **2013**, *13*, 3853−3861.
(44) Wijeratne, A. B.; Wijesundera, D. N.; Paulose, M.; Ahiabu, I. B.; Chu, W.-K.; Varghese, O. K.; Greis, K. D. Phosphopeptide separation using radially aligned titania nanotubes on titanium wire. *ACS Appl. Mater. Interfaces* **2015**, *7*, 11155−11164.
(45) Shrestha, N. K.; Macak, J. M.; Schmidt-Stein, F.; Hahn, R.; Mierke, C. T.; Fabry, B.; Schmuki, P. Magnetically Guided Titania Nanotubes for Site-Selective Photocatalysis and Drug Release. *Angew. Chem., Int. Ed.* **2009**, *48*, 969−972.
(46) Brunauer, S.; Emmett, P. H.; Teller, E. Adsorption of gases in multimolecular layers. *J. Am. Chem. Soc.* **1938**, *60*, 309−319.
(47) Barrett, E. P.; Joyner, L. G.; Halenda, P. P. The determination of pore volume and Area distributions in porous substances. I. Computations from nitrogen isotherms. *J. Am. Chem. Soc.* **1951**, *73*, 373−380.
(48) Harkins, W. D.; Jura, G. Surfaces of solids. XIII. A vapor adsorption method for the determination of the area of a solid without the assumption of a molecular area, and the areas occupied by nitrogen and other molecules on the surface of a solid. *J. Am. Chem. Soc.* **1944**, *66*, 1366−1373.
(49) Huyer, G.; Liu, S.; Kelly, J.; Moffat, J.; Payette, P.; Kennedy, B.; Tsaprailis, G.; Gresser, M. J.; Ramachandran, C. Mechanism of inhibition of protein-tyrosine phosphatases by vanadate and pervanadate. *J. Biol. Chem.* **1997**, *272*, 843−851.
(50) Thingholm, T. E.; Jensen, O. N.; Robinson, P. J.; Larsen, M. R. SIMAC (Sequential Elution from IMAC), a phosphoproteomics strategy for the rapid separation of monophosphorylated from multiply phosphorylated peptides. *Mol. Cell. Proteomics* **2008**, *7*, 661−671.
(51) Li, Q.-r.; Ning, Z.-b.; Tang, J.-s.; Nie, S.; Zeng, R. Effect of peptide-to-TiO_2 beads ratio on phosphopeptide enrichment selectivity. *J. Proteome Res.* **2009**, *8*, 5375−5381.
(52) Franc, V.; Řehulka, P.; Medda, R.; Padiglia, A.; Floris, G.; Šebela, M. Analysis of the glycosylation pattern of plant copper amine oxidases by MALDI-TOF/TOF MS coupled to a manual chromatographic separation of glycans and glycopeptides. *Electrophoresis* **2013**, *34*, 2357−2367.
(53) Rehulka, P.; Zahradnikova, M.; Rehulkova, H.; Dvorakova, P.; Nenutil, R.; Valik, D.; Vojtesek, B.; Hernychova, L.; Novotny, M. V. Microgradient separation technique for purification and fractionation of permethylated N-glycans before mass spectrometric analyses. *J. Sep. Sci.* **2018**, *41*, 1973−1982.
(54) R Core Team. *R: A language and environment for statistical computing*. R Foundation for Statistical Computing, Vienna, Austria. URL https://www.R-project.org/ (Last accessed: Jan 14, 2018)
(55) Lee, A.; Yang, H.-J.; Lim, E.-S.; Kim, J.; Kim, Y. Enrichment of phosphopeptides using bare magnetic particles. *Rapid Commun. Mass Spectrom.* **2008**, *22*, 2561−2564.
(56) Courcelles, M.; Frémin, C.; Voisin, L.; Lemieux, S.; Meloche, S.; Thibault, P. Phosphoproteome dynamics reveal novel ERK1/2 MAP kinase substrates with broad spectrum of functions. *Mol. Syst. Biol.* **2013**, *9*, 669.
(57) Kettenbach, A. N.; Gerber, S. A. Rapid and Reproducible Single-Stage Phosphopeptide Enrichment of Complex Peptide Mixtures: Application to General and Phosphotyrosine-Specific Phosphoproteomics Experiments. *Anal. Chem.* **2011**, *83*, 7635−7644.
(58) Connor, P. A.; McQuillan, A. J. Phosphate adsorption onto TiO_2 from aqueous solutions: An in situ internal reflection infrared spectroscopic study. *Langmuir* **1999**, *15*, 2916−2921.
(59) Engholm-Keller, K.; Larsen, M. R. Titanium dioxide as chemo-affinity chromatographic sorbent of biomolecular compounds applications in acidic modification-specific proteomics. *J. Proteomics* **2011**, *75*, 317−328.
(60) Krenkova, J.; Foret, F. Iron oxide nanoparticle coating of organic polymer-based monolithic columns for phosphopeptide enrichment. *J. Sep. Sci.* **2011**, *34*, 2106−2112.
(61) Balaur, E.; Macak, J. M.; Tsuchiya, H.; Schmuki, P. Wetting Behaviour of Layers of TiO_2 Nanotubes with Different Diameters. *J. Mater. Chem.* **2005**, *15*, 4488−4491.

DOI: 10.1021/acsomega.9b00571
ACS Omega 2019, 4, 12156−12166